

Robustly Safe Charging for Wireless Power Transfer

Haipeng Dai* Yang Zhao* Guihai Chen* Wanchun Dou* Chen Tian* Xiaobing Wu† Tian He‡

State Key Laboratory for Novel Software Technology, Nanjing University, Nanjing, Jiangsu 210024, CHINA

Wireless Research Centre, University of Canterbury, Private Bag 4800, Christchurch 8140, New Zealand

Computer Science and Engineering, University of Minnesota, Minneapolis, MN 55455, USA

{haipengdai, gchen, douwc, tianchen}@nju.edu.cn, yangzhao@mail.nju.edu.cn, barrywuh@gmail.com, tianhe@cs.umn.edu

Abstract—One critical issue for wireless power transfer is to avoid human health impairments caused by electromagnetic radiation (EMR) exposure. The existing studies mainly focus on scheduling wireless chargers so that (expected) EMR at any point in the area doesn't exceed a threshold R_t . Nevertheless, they overlook the EMR jitter that leads to exceeding of R_t even if the expected EMR is no more than R_t . This paper studies the fundamental problem of **RObustly SaFe** charging for wireless power transfer (ROSE), that is, scheduling the power of chargers so that the charging utility for all rechargeable devices is maximized while the probability that EMR anywhere doesn't exceed R_t is no less than a given confidence. We first build our empirical probabilistic charging model and EMR model. Then, we present EMR approximation and area discretization techniques to formulate ROSE into a Second-Order Cone Program, and the first redundant second-order cone constraints reduction algorithm to reduce the computational cost, and therefore obtain a $(1 - \epsilon)$ -approximation centralized algorithm. Further, we propose a $(1 - \epsilon)$ -approximation fully distributed algorithm scalable with network size for ROSE. Simulations and field experiments show that our algorithms can outperform comparison algorithms by 480.19%.

I. INTRODUCTION

Wireless Power Transfer (WPT) technology, which enables a wireless charger to transmit power to a rechargeable device across the air gap, has drawn increasing attention from both industrial and academic circles due to its merits of no wiring, reliability, ease of maintenance, *etc.* As per a recent report, wireless power transmission market is estimated to rise to 17.04 billion till 2020 [1]. Nevertheless, WPT typically incurs high electromagnetic radiation (EMR), which causes risks of tissue impairment, brain tumor, miscarriage, and detrimental impact on children that can be ten times greater than adults [2]. Therefore, it is a critical issue for WPT technology to avoid human health impairments caused by EMR exposure.

In this paper, we for the first time consider the jitter phenomenon of EMR aroused by wireless chargers. For illustration, Figure 1 shows that the measured charging power (which is exactly proportional to the EMR there) that a wireless rechargeable sensor node harvested from an off-the-shelf TX91501 power transmitter produced by Powercast [3] varies in a range, rather than keeping constant, for a fixed distance between 0.5 m and 1.8 m. Figure 2 shows the charging power histogram for the distance of 0.9 m. We can see that the charging power distribution basically matches a Gaussian distribution. Our quantitative evaluation based on Anderson-Darling test and Kolmogorov-Smirnov test also supports this observation. Essentially, EMR jitter is mainly due to the fading effect [4] caused by multipath propagation, shadowing from obstacles, *etc.* Thereby, the resulted EMR is indeed the superposition of multiple copies of that for

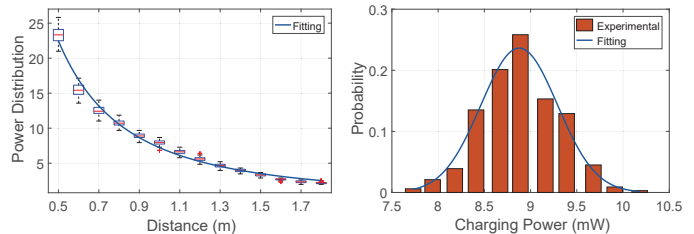


Fig. 1: Charging power distribution with distance

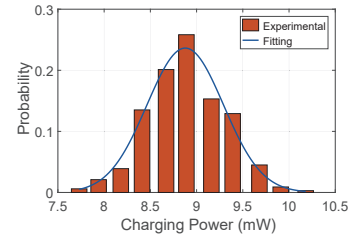


Fig. 2: Charging power for distance of 0.9 m with one single charger

the transmitted signal, each traversing a different path with different attenuation, delay and phase shift, resulting in either constructive or destructive interference. Thus, we argue that it is not sufficient to guarantee the traditional EMR safety, which we call *deterministic EMR safety*, as done by most existing wireless charging schemes; that is, the (expected) EMR intensity anywhere should not exceed a threshold, say R_t . The main reason is that even if the expected EMR is no more than R_t , it is always possible that EMR exceeds R_t and the corresponding probability can be up to 50%; and traditional schemes cannot distinguish between the harmful levels of two EMR distributions with different jitter amplitudes but same average value, which are definitely different. One may argue that why not take the maximum observed EMR in history for a charger to build a new “maximum EMR model”, and therefore directly use existing schemes for ensuring deterministic EMR safety. Our answer is no for the following reasons. First, due to the probabilistic nature of EMR, one can never guarantee that the maximum EMR in the future must not surpass the maximum one in history; rather, using a confidence level for future prediction based on a probabilistic model built upon history data should be more appropriate. Second, the maximum endurable intensity for instantaneous or short-term EMR is shown to be much higher than the average endurable EMR. As per the standards published by ICNRP [5] in Europe and the regulation GB8702-2014 in China [6], for example, the maximum allowed instantaneous electric field intensity is 32 times of its corresponding maximum allowed average value. Thus, occasional violation of traditional EMR threshold is not unacceptable; instead, the issue matters here is to control the frequency of occurrence of such violation. Third, this solution might be too conservative to use in practical applications, as to satisfy the more stringent EMR constraints, chargers need to be scheduled at lower levels, yielding lower charging utility. Consequently, to better characterize the EMR safety extent given its probabilistic nature, we propose the notion of *probabilistic EMR safety* that requires the probability that EMR intensity anywhere does not exceed a given threshold R_t should be no less than a given confidence η ($0 < \eta \leq 1$).

We are concerned with the problem of RObustly Safe charging for wireless power transfer (ROSE) in this paper. We first propose probabilistic charging and EMR models to capture their jitter nature. By defining charging utility of a device to be proportional to its received power, our optimization goal is to maximize the aggregated (expected) charging utility for all devices. Formally, given a number of static wireless chargers and rechargeable devices on a 2D plane, our problem is to schedule the power of chargers so that the overall charging utility for all the devices is maximized while the probability that EMR intensity at any point in the plane does not exceed a given threshold R_t is no less than a given confidence η .

Though there have emerged some works [2], [7]–[14] considering EMR safety, none of them considers the jitter property of EMR and thus cannot apply to address ROSE. Moreover, their solutions are essentially based on either discrete optimization or linear programming methods, which are fundamentally different from ours. The other works consider charging efficiency issues for wireless charger networks [15]–[17], but none of them takes into account the EMR safety.

The main technical challenges for ROSE are four-folds. The first challenge is that the ROSE problem is nonlinear and NP-hard. ROSE is nonlinear because both the charging power and EMR for chargers are probabilistic and nonlinear; the probabilistic EMR safety requirement is imposed on every point in the plane which implies an infinite number of constraints. The second challenge is due to the high computational cost of the centralized algorithm. Even if we could approximately transform the infinite constraints of the problem into limited ones, their number is still huge and causes high computational cost. The third challenge is to design a fully distributed algorithm. As generally neighboring chargers have overlapping area for power transfer and caused EMR, the optimization of power scheduling for all chargers is inevitably correlated. We need to decouple such correlation, and make the treatments of the nonlinear problem distributed. The fourth challenge is to bound the performance for the distributed algorithm. We need to evaluate the caused performance loss when we reduce its infinite nonlinear constraints to finite ones and when we make the algorithm distributed.

We propose both centralized and distributed algorithms by addressing the four challenges one by one. First, we transform the probabilistic constraint of ROSE into a second-order cone one, and propose EMR approximation and area discretization techniques to reformulated ROSE as a traditional Second-Order Cone Program (SOCP), which can be optimally addressed by convex optimization techniques such as interior point methods [18]. Second, we propose the first redundant second-order cone constraints reduction scheme to effectively remove the redundant constraints. Third, we present an area partition scheme which basically divides the area into many subareas and considers the optimization problem in each sub-area independently. This is the first fully distributed algorithm for SOCP that is scalable with network size. Note that we also propose the first distributed redundant second-order cone constraints reduction scheme to reduce computational cost. Fourth, by controlling the error for the EMR approximation and area discretization, and the granularity of the distributed area partition scheme, we prove that our distributed algorithm achieves $(1 - \epsilon)$ -approximation ratio.

We conducted both simulations and field experiments to evaluate our proposed algorithms. The results show that our algorithms can outperform comparison algorithms by 480.19%.

II. RELATED WORK

To the best of our knowledge, we are the first to study the robustly safe charging problem that considers the jitter of aroused EMR of wireless chargers. First, there exist some works [2], [7]–[14] studying on wireless charging issues with EMR safety concern, but none of them considers the EMR jitter phenomenon. For example, Dai *et al.* initiated the study of safe charging by first taking the detrimental effect of high EMR into consideration in [2]. They investigated how to schedule unadjustable chargers [2], [7] and adjustable chargers [8], [9] to maximize the overall charging utility of all rechargeable devices. Dai *et al.* also proposed the first charger deployment scheme for wireless chargers with EMR safety concern [11], and considered radiation constrained scheduling of wireless charging tasks in [12], [13]. All these schemes merely consider deterministic EMR safety and cannot be applied to address our problem. Besides, their solutions are essentially based on either discrete optimization or linear programming methods, which differ from ours that relies on quadratic programming.

Second, some other works study charging efficiency issues for wireless charger networks but overlook the EMR safety [15]–[17]. For example, Dai *et al.* presented the directional charging problem where both the charging area for chargers and receiving area for devices can be modeled as sectors, and studied omnidirectional charging using directional chargers in [16], and the wireless charger placement problem in [17].

III. PROBLEM FORMULATION

A. Preliminaries

Suppose there are n identical wireless chargers $S = \{s_i\}_{i=1}^n$ and m identical rechargeable devices $O = \{o_j\}_{j=1}^m$ located in a 2D plane Ω . With a little abuse of notation, we still use s_i (and o_j) to denote the position of wireless charger s_i (and device o_j). We build our probabilistic charging model based on the omnidirectional charging model proposed in [2], [15] for chargers and devices, that is, both of the power charging area of chargers and the power receiving area of devices are in the shape of a disk. We stress that our analytical results can be directly extended to the directional charging models [16], [17]. Table I lists the notations used in this paper.

We establish our probabilistic model based on the field experiments using the off-the-shelf TX91501 power transmitters and wireless rechargeable sensor nodes produced by Powercast [3]. We used a sensor node to receive power from a single TX91501 power transmitter at a distance from $0.5m$ to $1.8m$. We first fit the distribution of the node's received power at a certain distance into a Gaussian distribution, and then fit the distribution of the expectation (and the standard deviation) of the fitted Gaussian distribution at all measured distances to a nearly inverse-square function. Figure 1 and 3 show the fitting results of the expectation and standard deviation of the received power for the node. In addition, to qualitatively measure the goodness of Gaussian distribution fitting, we use Anderson-Darling test (A-D test) and Kolmogorov-Smirnov test (K-S test), which are statistical tests of whether a given sample of data is drawn from a given probability distribution [19]. Our experimental results show that the probability value, or p -value, for both the tests can be up to 0.0624, which is

TABLE I: Notations

Symbol	Description
s_i	i -th wireless charger (or its position)
o_j	j -th rechargeable device (or its position)
n	Number of wireless chargers
m	Number of rechargeable devices
$P(\cdot)$	Charging power function
α_1, β_1	Constants in the expression of charging power expectation
α_2, β_2	Constants in the expression of charging power standard deviation
D	Charging radius for wireless chargers
x_i	Adjusting factor of the i -th wireless charger
$\bar{P}(d), \sigma_P(d)$	Expectation and standard deviation of charging power with distance d
$\bar{e}(d), \sigma_e(d)$	Expectation and standard deviation of EMR with distance d
c_e	Constant in the EMR model
c_u	Constant in the charging utility model
$\mathcal{U}(\cdot)$	Utility function
R_t	EMR threshold
η	Confidence
$\bar{P}_{iz}, \tilde{\sigma}_{P,iz}$	Approximated expectation and standard deviation of EMR in subarea \mathcal{A}_z from s_i
$\mathbf{N}(s_i)$	Neighbor set of charger s_i

larger than the commonly used significance level of 0.05 and thus passes both the tests. For similar experiments with two chargers, Figure 4 shows that the p -value for both the tests is dramatically improved, and its mean value becomes larger than 0.13. This indicates that our Gaussian distribution fitting is more appropriate for realistic cases with multiple chargers. Note that though some works claim that WPT channels can be characterized by log-normal fading in some cases [20], [21], our empirical results show that Gaussian distribution fitting achieves comparable or higher p -value compared with log-normal distribution fitting. After all, Gaussian distribution can well approximate log-normal distribution if $\mu > 6\sigma$ [22], while we have $\mu > 16\sigma$ in our case. To sum up, the maximum charging power for a single charger at distance d is:

$$P(d) \begin{cases} \sim \mathcal{N}\left(\frac{\alpha_1}{(d+\beta_1)^2}, \left[\frac{\alpha_2}{(d+\beta_2)^2}\right]^2\right), & 0 \leq d \leq D \\ = 0, & d > D \end{cases}$$

where $\alpha_1, \beta_1, \alpha_2$, and β_2 are four constants, d is the distance between s_i and o_j , and D is the charging radius. For convenience, we define $\bar{P}(d) = \mathbf{E}[P(d)] = \frac{\alpha_1}{(d+\beta_1)^2}$ and $\sigma_P(d) = \sqrt{\mathbf{Var}[P(d)]} = \frac{\alpha_2}{(d+\beta_2)^2}$, and then $P(d) \sim \mathcal{N}(\bar{P}(d), \sigma_P(d)^2)$ for $0 \leq d \leq D$, and $P(d) = 0$ for $d > D$. Moreover, we define adjusting factor x_i ($0 \leq x_i \leq 1$) for charger s_i as the ratio of the adjusted working power to the maximum power, then the charging power at distance d becomes $P(d)x_i$. Further, we adopt the power additive model for multiple chargers [23], *i.e.*, the received power of a device o_j is the sum of the received power from all its surrounding chargers.

We adopt the electromagnetic radiation (EMR) model proposed in [2], [8], that is, the accumulated EMR at a point is the sum of the EMR caused by each charger which is proportional to the corresponding charging power.

$$e(p) = c_e \sum_{i=1}^n P(d(s_i, p))x_i. \quad (1)$$

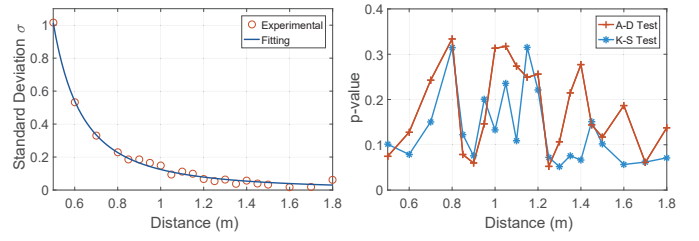


Fig. 3: Fitting result for stan- Fig. 4: A-D test and K-S test. c_e is a predetermined constant and $d(s_i, p)$ is the distance from charger s_i to point p .

For the charging utility model, we adopt the linear model proposed in [8], namely

$$\mathcal{U}(x) = c_u \cdot x, \quad (2)$$

where c_u is a predetermined constant and x denotes the received power.

B. Problem Statement

Let $d(s_i, o_j)$ be the distance from charger s_i to device o_j . Considering the jitter of the received power of device o_j from charger s_i , *i.e.*, $P(d(s_i, o_j))x_i$, we take the expected charging utility over time $\mathbf{E}[\mathcal{U}(P(d(s_i, o_j))x_i)] = \mathbf{E}[c_u P(d(s_i, o_j))x_i] = c_u \bar{P}(d(s_i, o_j))x_i$ for optimization. Therefore, the optimization goal for ROSE is to maximize the aggregate expected charging utility of all devices, *i.e.*, $c_u \sum_{i=1}^n \sum_{j=1}^m \bar{P}(d(s_i, o_j))x_i$. As for the constraint, we require that for any point $p \in \mathbb{R}^2$, the probability that the aggregated EMR there doesn't exceed a given threshold R_t is not less than a given confidence η ($0 < \eta \leq 1$), *i.e.*, $\mathbf{Prob}(c_e \sum_{i=1}^n P(d(s_i, p))x_i \leq R_t) \geq \eta$. To sum up, the problem of RObustly SafE charging for wireless power transfer (ROSE) can be defined as follows

$$\begin{aligned} (\mathbf{P1}) \quad & \max_{x_i} \quad c_u \sum_{i=1}^n \sum_{j=1}^m \bar{P}(d(s_i, o_j))x_i \\ \text{s.t.} \quad & \forall p \in \mathbb{R}^2, \quad \mathbf{Prob}(c_e \sum_{i=1}^n P(d(s_i, p))x_i \leq R_t) \geq \eta, \\ & 0 \leq x_i \leq 1 \quad (i = 1, \dots, n). \end{aligned} \quad (3)$$

Note that x_i s are the optimization variables. Because the sum of independent Gaussian random variables also follows Gaussian distribution and its expectation and variance is exactly the sum of the expectation and variance of all the Gaussian random variables, respectively [24], we let $P = \sum_{i=1}^n P(d(s_i, p))x_i$ and $\sigma_P^2 = \sum_{i=1}^n \sigma_P^2(d(s_i, p))x_i^2$, and introduce an assistant zero mean unit variance Gaussian variable, the constraint in the former formulation can be rewritten as

$$\begin{aligned} & \mathbf{Prob}\left(\frac{P - \mathbf{E}[P]}{\sigma_P} \leq \frac{R_t/c_e - \mathbf{E}[P]}{\sigma_P}\right) \\ & = \mathbf{Prob}\left(\frac{P - \mathbf{E}[P]}{\sigma_P} \leq z\right) \geq \eta. \end{aligned} \quad (4)$$

Suppose $\Phi(z) = \frac{1}{\sqrt{2\pi}} \int_{-\infty}^z e^{-t^2/2} dt$ is the cumulative distribution function of a zero mean unit variance Gaussian random variable, then we have $\frac{R_t/c_e - \mathbf{E}[P]}{\sigma_P} \geq \Phi^{-1}(\eta)$. By rearranging the inequality and plugging in the expressions of P and σ_P , we have

$$\sum_{i=1}^n \bar{P}(d(s_i, p))x_i + \Phi^{-1}(\eta) \sqrt{\sum_{i=1}^n \sigma_P^2(d(s_i, p))x_i^2} \leq \frac{R_t}{c_e}, \quad (5)$$

which is exactly in the form of second-order cone constraint, a special type of quadratic constraints [18]. Consequently, the formulation **P1** can be equivalently transformed into

$$\begin{aligned}
 (\mathbf{P2}) \quad & \max_{x_i} \quad c_u \sum_{i=1}^n \sum_{j=1}^m \overline{P}(d(s_i, o_j))x_i \\
 \text{s.t.} \quad & \sum_{i=1}^n \overline{P}(d(s_i, p))x_i + \Phi^{-1}(\eta) \sqrt{\sum_{i=1}^n \sigma_P^2(d(s_i, p))x_i^2} \leq \frac{R_t}{c_e}, \\
 & \forall p \in \mathbb{R}^2, 0 \leq x_i \leq 1 \quad (i = 1, \dots, n). \quad (6)
 \end{aligned}$$

Since the constraint of **P1** is nonlinear and continuous, ROSE falls in the realm of nonlinear programs, which are generally NP-hard [25]. Then we have the following theorem. Note that we omit some proofs in this paper to save space.

Theorem 3.1: The ROSE problem is NP-hard.

IV. $(1 - \epsilon)$ -APPROXIMATION CENTRALIZED ALGORITHM

In this section, we present a centralized algorithm that achieves $(1 - \epsilon)$ -approximation ratio to address ROSE. First, we use two piecewise constant functions to approximate the nonlinear expectation and standard deviation of EMR value with distance, respectively, and thus partition the whole 2D plane into multiple subareas and the aggregated EMR for any point in a given subarea is the same. Consequently, we reformulate ROSE into a traditional Second-Order Cone Program (SOCP), which can be optimally addressed. Second, considering the high time complexity caused by the huge number of second-order cone constraints in the reformulated SOCP, we propose a centralized algorithm to eliminate the redundant constraints that can be safely removed without hurting the final results.

A. Piecewise Constant Approximations for EMR and Area Discretization

We use two piecewise constant functions to approximate the nonlinear expectation and standard deviation of EMR, which are denoted by $\bar{e}(d)$ and $\sigma_e(d)$, respectively. Note that we have $\bar{e}(d) = c_e \frac{\alpha_1}{(d + \beta_1)^2}$ and $\sigma_e(d) = c_e \frac{\alpha_2}{(d + \beta_2)^2}$. The sets of endpoints of the piecewise constant line segments for these two functions are exactly the same, which are denoted by $\ell(1), \dots, \ell(Q)$ ($\ell(0) = 0, \ell(Q) = D$) in order of distance. Next, we plot Q concentric circles with radii of $\ell(1), \dots, \ell(Q)$, respectively, for each charger, and thereby partition the whole 2D plane into multiple subareas that are shaped by these concentric circles. One key observation here is that for each formed subarea, either the approximated expectation or the standard deviation of EMR generated by a charger is the same for any point in the considered subarea, and so is the case for aggregated EMR from multiple chargers. Figure 5 shows an example for which we draw two concentric circles for three chargers with radius $\ell(1)$ and $\ell(2)$, and obtain 12 subareas.

Given two established error thresholds, say ϵ_1 and ϵ_2 , we can set the values of Q and $\ell(1), \dots, \ell(Q)$ as follows.

Lemma 4.1: By setting $\ell(0) = 0$,

$$\ell(q) = \min\{\sqrt{1 + \epsilon_1} \cdot [\ell(q-1) + \beta_1], \sqrt{1 + \epsilon_2} \cdot [\ell(q-1) + \beta_2]\}, \quad (7)$$

where $q = 1, \dots, Q - 1$ and $\ell(Q) = D$ where Q satisfies

$$\ell(Q-1) < D \leq \min\{\sqrt{1 + \epsilon_1} \cdot [\ell(Q-1) + \beta_1], \sqrt{1 + \epsilon_2} \cdot [\ell(Q-1) + \beta_2]\}, \quad (8)$$

and using the following piecewise constant functions $\tilde{e}(d)$

$$\tilde{e}(d) = \begin{cases} \bar{e}(0), & d = 0 \\ \bar{e}(\ell(q-1)), & \ell(q-1) < d \leq \ell(q) \quad (q = 1, \dots, Q) \\ 0, & d > D, \end{cases} \quad (9)$$

and

$$\tilde{\sigma}_e(d) = \begin{cases} \sigma_e(0), & d = 0 \\ \sigma_e(\ell(q-1)), & \ell(q-1) < d \leq \ell(q) \quad (q = 1, \dots, Q) \\ 0, & d > D, \end{cases} \quad (10)$$

the approximation errors of EMR expectation and standard deviation by a single charger from distance d satisfy

$$1 \leq \frac{\tilde{e}(d)}{\bar{e}(d)} \leq 1 + \epsilon_1. \quad (11)$$

and

$$1 \leq \frac{\tilde{\sigma}_e(d)}{\sigma_e(d)} \leq 1 + \epsilon_2. \quad (12)$$

B. Problem Reformulation

Consequently, let \tilde{P}_{iz} and $\tilde{\sigma}_{P,iz}$ be the corresponding approximated expectation and standard deviation of charging power at the z -th subarea in all Z subareas when the adjusting factors for all chargers are 1, **P2** can be reformulated as

$$\begin{aligned}
 (\mathbf{P3}) \quad & \max_{x_i} \quad c_u \sum_{i=1}^n \sum_{j=1}^m \overline{P}(d(s_i, o_j))x_i \\
 \text{s.t.} \quad & \sum_{i=1}^n \tilde{P}_{iz}x_i + \Phi^{-1}(\eta) \sqrt{\sum_{i=1}^n \tilde{\sigma}_{P,iz}^2 x_i^2} \leq \frac{R_t}{c_e}, \quad (z = 1, \dots, Z) \\
 & 0 \leq x_i \leq 1, \quad (i = 1, \dots, n). \quad (13)
 \end{aligned}$$

The above formulation falls exactly into the realm of Second-Order Cone Program (SOCP), which can be optimally addressed by convex optimization techniques such as interior point methods [18]. We have the following lemma.

Lemma 4.2: Any feasible solution to problem **P3** is also feasible to problem **P2**.

Apparently, the time complexity of solving problem **P3** is positively related to the number of its second-order cone constraints. To alleviate the computational cost, we will discuss how to eliminate useless constraints in the next subsection.

C. Centralized Redundant Constraint Reduction

To begin with, we give the following formal definition.

Definition 4.1: (Redundant second-order cone constraint) Consider the system with n variables and m second-order cone constraints:

$$\|A_i x + b_i\|_2 \leq c_i^T x + d_i, \quad i \in \{1, \dots, m\} \quad (14)$$

where $A_i \in \mathbb{R}^{n_i \times n}$, $b_i \in \mathbb{R}^{n_i}$, $x \in \mathbb{R}^n$, and $d_i \in \mathbb{R}$. The feasible region S associated with the system is defined as

$$S \triangleq \{x \in \mathbb{R}^n \mid \|A_i x + b_i\|_2 \leq c_i^T x + d_i, \quad i \in \{1, \dots, m\}\}. \quad (15)$$

Moreover, for any fixed $k \in \{1, \dots, m\}$, define the feasible region by

$$S_k \triangleq \{x \in \mathbb{R}^n \mid \|A_i x + b_i\|_2 \leq c_i^T x + d_i, \quad i \in \{1, \dots, m\} \setminus k\}. \quad (16)$$

Then, the k -th constraint $\|A_k x + b_k\|_2 \leq c_k^T x + d_k$ ($1 \leq k \leq m$) is a redundant constraint if and only if $S_k = S$.

Essentially, the redundant second-order cone constraints are those constraints that can be safely removed without affecting the feasible region of the SOCP problem. As there is no algorithm available for redundant second-order cone constraint identification and reduction, we propose the first scheme to address this problem. In particular, this method consists of three steps: (1) It identifies and eliminates those trivial constraints that can be always satisfied even all x_i s set to be 1; (2) it compares each pair of constraints, and removes the constraint that has both the coefficients of \tilde{P}_{iz} and $\tilde{\sigma}_{P,iz}$ being less than that of the other constraint, respectively, for each optimization variable x_i ($i = 1, \dots, n$); (3) it picks the constraints one by one; and for each constraint, it takes the formula at the left-hand side (L.H.S.) of the constraint as the optimization function and uses the other constraints to compute an optimal solution. If the solution is no more than the constant at the right-hand side (R.H.S.) of the considered constraint, which means the constraint will always be satisfied in the presence of the other constraints, then the constraint is redundant and can be removed; otherwise cannot. In our problem, suppose the k -th constraint is chosen, and the optimization program is shown as below.

$$\begin{aligned} \max_{x_i} \quad & \sum_{i=1}^n \tilde{P}_{ik} x_i + \Phi^{-1}(\eta) \sqrt{\sum_{i=1}^n \tilde{\sigma}_{P,ik}^2 x_i^2} \\ \text{s.t.} \quad & \sum_{i=1}^n \tilde{P}_{iz} x_i + \Phi^{-1}(\eta) \sqrt{\sum_{i=1}^n \tilde{\sigma}_{P,iz}^2 x_i^2} \leq \frac{R_t}{c_e}, \\ & (z = 1, \dots, Z; z \neq k) \\ & 0 \leq x_i \leq 1, \quad (i = 1, \dots, n). \end{aligned} \quad (17)$$

The above formulation is hard to deal with, so we introduce an assist variable y and rewrite the formulation as

$$\begin{aligned} \max_{x_i} \quad & \sum_{i=1}^n \tilde{P}_{ik} x_i + y \\ \text{s.t.} \quad & \sum_{i=1}^n \tilde{P}_{iz} x_i + \Phi^{-1}(\eta) \sqrt{\sum_{i=1}^n \tilde{\sigma}_{P,iz}^2 x_i^2} \leq \frac{R_t}{c_e}, \\ & (z = 1, \dots, Z; z \neq k) \\ & \Phi^{-1}(\eta) \sqrt{\sum_{i=1}^n \tilde{\sigma}_{P,ik}^2 x_i^2} - y = 0, \\ & 0 \leq x_i \leq 1, \quad (i = 1, \dots, n). \end{aligned} \quad (18)$$

This formulation is slightly different with the traditional expression of SOCP [18] because it has equality constraints. Nevertheless, we can equivalently transform each second-order constraint to a quadratic one, and then use KKT conditions [18] to compute an optimal solution. After obtaining the optimal solution, we check whether it exceeds $\frac{R_t}{c_e}$. If not, we identify the constraint as a redundant one and remove it.

For simplicity, we still use **P3** to express the problem after the redundant constraint reduction if no confusion arises.

D. Theoretical Analysis

Theorem 4.1: Setting $\epsilon_1 = \epsilon_2 = \epsilon$, the centralized algorithm for ROSE achieves $(1 - \epsilon)$ -approximation ratio, and its time complexity is $O(n^5 \epsilon^{-3})$.

V. $(1 - \epsilon)$ -APPROXIMATION FULLY DISTRIBUTED ALGORITHM

In this section, we develop a $(1 - \epsilon)$ -approximation algorithm for ROSE. First, we make the area discretization algorithm in the centralized algorithm distributed. Second, we propose the first distributed redundant second-order cone constraint reduction algorithm to remove redundant constraints. Third, we present a distributed algorithm to address SOCP. To the best of our knowledge, it is the first fully distributed algorithm for SOCP that is scalable with network size.

A. Distributed EMR Approximation, Area Discretization, and Redundant Constraint Reduction

Assume that each charger already knows the parameters regarding probabilistic charging model, EMR model, and approximation error threshold, it is then able to independently conduct the EMR approximation. Further, let neighbor set $\mathbf{N}(s_i)$ be the set of chargers having non-empty intersected coverage area with s_i . Apparently, each charger can communicate with the chargers in its neighbor set for their position information to implement area discretization. Next, as there are no prior works regarding distributed redundant second-order cone constraint reduction, we develop the first algorithm to address this problem. We only sketch the algorithm due to space limit. A charger running this algorithm first locally removes trivial constraints by using the centralized redundant second-order cone constraint reduction algorithm. Then, it exchanges the obtained constraints with neighbors in two-hops, picks out the constraints that involve itself, and then performs the centralized redundant second-order cone constraint reduction algorithm one more time. We can prove that this algorithm achieves the same performance as its centralized version.

B. Distributed SOCP Algorithm

We propose a distributed algorithm to address SOCP in this subsection. The key intuitions of the algorithm are as follows. First, to decompose the problem into multiple minor ones that can be locally addressed, we propose a new area partition scheme to partition the whole area into many smaller subareas. Especially, we preserve ‘‘blank strips’’ between the subareas by switching off the chargers in these strips so that the impact of charging power together with EMR from chargers in neighboring subareas can be eliminated. By this means, we can safely consider each subarea independently of others. Second, to avoid unexpected performance loss caused by adopting a specific area partition strategy and thus bound the overall performance, we enumerate all area partition strategies to forge a solution that is globally feasible and has performance guarantee. The whole distributed framework needs only one-round information gathering and one-round dissemination that involves chargers within a certain constant distance.

Algorithm 1 shows the details of the whole distributed algorithm running at each charger s_i . After initialization, Algorithm 1 first partitions the whole area into multiple uniform grid cells with side length of $2D$ where D is the charging radius for wireless chargers, and further groups these cells into larger squares called *M-Clusters*, each of which contains $M \times M$ cells where $M = \left\lceil \frac{1 + \sqrt{1 - \epsilon/2}}{\epsilon/2} \right\rceil$. This process can be implemented locally at each charger s_i based on its geographical location. Further, each charger participates in electing a *cell*

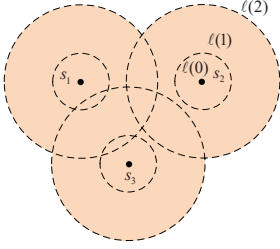
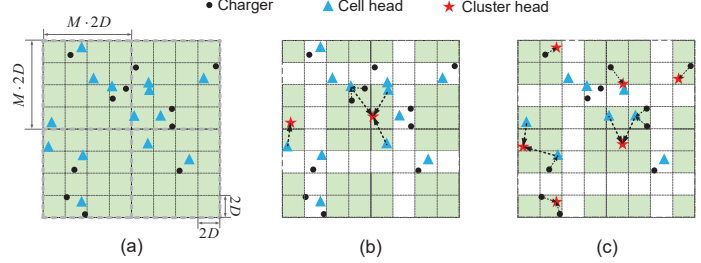


Fig. 5: Area discretization


 Fig. 6: M -Clusters, $(M - 1)$ -Clusters for $\langle 2, 2 \rangle$ and $\langle 3, 3 \rangle$

Algorithm 1: Distributed Algorithm for ROSE at Charger s_i

- Input:** Charger set S , device set O , EMR threshold R_t , confidence η , and error threshold ϵ
- Output:** Adjusting factor x_i
- 1 Apply distributed area discretization technique based on the collected information from neighbor set $\mathbf{N}(s_i)$ with approximation error thresholds for EMR expectation and standard deviation of $\epsilon/2$, and then compute the approximated expectation $\tilde{P}_{k,z}$ and standard deviation $\tilde{\sigma}_{P,k,z}$ in each subarea \mathcal{A}_z for each charger $s_k \in s_i \cup \mathbf{N}(s_i)$;
 - 2 Apply distributed redundant second-order cone constraint reduction algorithm to remove redundant constraints;
 - 3 Set $M = \left\lceil \frac{1 + \sqrt{1 - \epsilon/2}}{\epsilon/2} \right\rceil$;
 - 4 Identify itself as a member of a certain cell based on its stored geographical information;
 - 5 Take part in electing a cell head in its cell;
 - 6 **if** s_i itself is a cell head **then**
 - 7 Participate in electing the cluster heads for all $(M - 1)$ -Clusters for different turn-off policies that is related to itself;
 - 8 **for All** $(M - 1)$ -Clusters for all turn-off policies that are related to it **do**
 - 9 **if** s_i itself is a cluster head **then**
 - 10 Collect all related information from all cell heads in the $(M - 1)$ -Cluster;
 - 11 Use the traditional SOCP algorithm to compute a solution;
 - 12 Send the solution to all the cell heads;
 - 13 **else**
 - 14 Send related information to its corresponding cluster head, and receive the adjusting factors for the chargers in its cell from the cluster head;
 - 15 Send the corresponding adjusting factors to all chargers located in its cell;
 - 16 **else**
 - 17 Send related information to its cell head, and receive $M \times M$ adjusting factors from the cell head;
 - 18 Compute the average value of the obtained $M \times M$ adjusting factors as the final solution.
-

head for its associated cell through methods such as voting. Figure 6(a) shows an instance for which the area is partitioned into 64 cells which in turn form 4 M -Clusters. Note that black dots denote normal chargers while blue triangles denote cell heads. Second, the algorithm further partitions the area using a so-called *turn-off* policy, which is formally defined as a tuple of $\langle p, q \rangle$. All M -Clusters that adopt a turn-off policy $\langle p, q \rangle$ will turn off all the chargers located in the cells that lie in their p -th row and q -th column, and thereby, the cells with active chargers are regrouped into new clusters with scale of no more than $(M - 1) \times (M - 1)$ cells, which we call $(M - 1)$ -Clusters. Next, cell heads in a $(M - 1)$ -Cluster interacts with each other to elect a *cluster head* which is responsible for the computing task for the whole cluster as well as information collection and dissemination. Figure 6(b) and

6(c) show the obtained 9 $(M - 1)$ -Clusters after carrying out turn-off policies $\langle 2, 2 \rangle$ and $\langle 3, 3 \rangle$, respectively, and in the figures red stars indicate cluster heads while directed dashed arrows indicate information flows with directions. Third, the algorithm enumerates all possible $M \times M$ different turn-off policies and accordingly obtains M^2 adjusting factors for each charger. Then, each charger computes the average value of these adjusting factors as the final solution.

Besides, though there have emerged a few distributed algorithms for SOCP, most of them are based on dual decomposition such as [26], and have no performance guarantee after a fixed number of iterations or do not scalable with network size under a given performance requirement. In contrast, our proposed algorithm has performance guarantee with a few constant steps, and is scalable with network size.

C. Performance Analysis

Theorem 5.1: *The output of Algorithm 1 for ROSE is a feasible solution to P3. Moreover, Algorithm 1 achieves $(1 - \epsilon)$ -approximation ratio in terms of the overall expected charging utility, and its communication delay is $O(\epsilon^{-1})$.*

Proof: Please see Appendix for the proof. ■

VI. SIMULATION RESULTS

In this section, we perform simulations to verify the performance of our proposed ROSE algorithms.

A. Evaluation and Baseline Setup

We use the following evaluation setup unless otherwise stated. The considered field is a $100m \times 100m$ square area. We set $\alpha_1 = 60$, $\beta_1 = 40$, $D = 13m$, $n = 30$, $\epsilon = 0.15$, $R_t = 0.08$, $\eta = 0.6$, $c_e = 1$, $c_u = 1$, $\alpha_2 = 50$, $\beta_2 = 20$, and $m = 1000$, respectively. Each data point in figures indicates an average result of 100 random topologies. We develop four algorithms for comparison as there are no existing approaches for ROSE. The first algorithm is Optimal, which approximates the optimal algorithm using our centralized ROSE algorithm with $\epsilon = 0.05$. The second is Set-Cover that borrows the idea from the traditional set-cover algorithm. Each time it greedily picks a charger that can be turned up to achieve the largest charging utility increment. The third (fourth) is 1/3 Approximation (1/4 Approximation) that divides the whole area into uniform hexagons (squares) with side length of $2D$ and elects a cell head in each individual hexagon (square) to run the centralized ROSE algorithm to obtain a solution and cut down it to 1/3 (1/4) to guarantee a global feasible solution.

B. Performance Comparison

1) *Impact of Charger Number n :* Our simulation results show that on average, Centralized ROSE outperforms Set-Cover, 1/3 Approximation, and 1/4 Approximation by 24.49%,

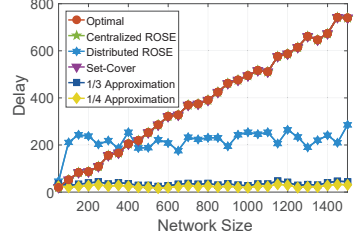
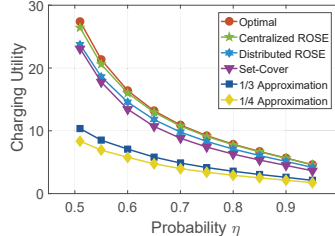
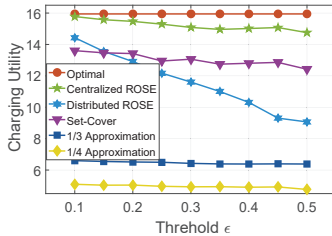
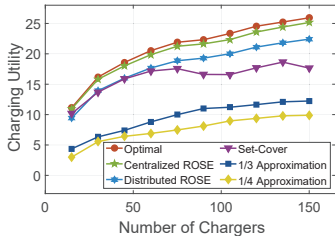


Fig. 7: n vs. charging utility Fig. 8: ϵ vs. charging utility

118.77%, and 177.23%, respectively, in terms of n . Figure 7 shows that basically the overall charging utility of all the algorithms increases with n , but the increasing trend slows down with n . Set-Cover algorithm demonstrates a slight fluctuation because of its heuristic charger selection strategy. The performance gap between Centralized ROSE and Optimal is as low as 3.07%, and Distributed ROSE has performance gain of at least 10.57% compared with Set-Cover, 1/3 Approximation, and 1/4 Approximation. Moreover, 1/3 Approximation and 1/4 Approximation have the worst performance due to their conservative cutting-down operation on the obtained solution.

2) *Impact of Error Threshold ϵ* : Our simulation results show that on average, Centralized ROSE outperforms Set-Cover, 1/3 Approximation, and 1/4 Approximation by 16.81%, 135.67%, and 207.18%, respectively, in terms of ϵ . Figure 8 shows that the charging utility of all the algorithms except Optimal gradually degrades with ϵ . Especially, Distributed ROSE decreases at a faster speed than others due to its adopted area partitioning scheme. The charging utility for both Centralized ROSE and Distributed ROSE is always larger than $1 - \epsilon$ of the optimal value, while that for 1/3 Approximation (1/4 Approximation) is larger than 1/3 (1/4) of the optimal one, which corroborates our theoretical results. In particular, even for $\epsilon = 0.5$, the performance of Centralized ROSE reaches 95.48% of that for Optimal.

3) *Impact of Confidence η* : Our simulation results show that on average, Centralized ROSE outperforms Set-Cover, 1/3 Approximation, and 1/4 Approximation by 21.43%, 125.63%, and 175.85%, respectively, in terms of η . Figure 9 shows that the charging utility for all the algorithms decreases with η , which makes sense as a more rigorous EMR safety requirement intuitively leads to a more conservative scheduling scheme and thus lower charger utility.

4) *Impact of network size on delay*: Our simulation results show that on average, the delay of Distributed ROSE keeps nearly constant as the network size scales up, and outperforms Optimal, Centralized ROSE, and Set-Cover by 72.55%. We fix the charger density to 0.002, and let the communication radius of chargers be twice the charging radius D . Figure 10 shows the network delay for Optimal, Centralized ROSE, and Set-Cover increases proportionally to the network size as they require network-wide information communication. In contrast, the delay for the other three algorithms keeps relatively stable when the network size exceeds 200 as they only need local communication within a subarea with a bounded size.

VII. FIELD EXPERIMENTS

We conducted field experiments to evaluate the performance of our algorithms. Figure 11 shows our testbed deployed in a $2.4\text{ m} \times 2.4\text{ m}$ square area that consists of eight TX91501 power transmitters and two rechargeable sensor nodes [27]–[33] both of which are produced by Powercast [34], an AP for data collection from sensor nodes, and a laptop connecting to

Fig. 9: η vs. charging utility Fig. 10: Delay vs. network size

the AP for data fetching and analysis. The eight chargers are deployed at the vertices and middle points of the edges of the square area with orientation angles 26.56° , 116.56° , 153.44° , 26.56° , 206.56° , 333.44° , 243.44° , and 206.56° , respectively. Note that these chargers are actually directional, whose charging area can be modeled as a sector with angle 60° and radius 4 m . Since the power of the chargers is not adjustable, we place a piece of copper foil tape with proper length, width, position, and bending angle in front of each charger so that the charging power and EMR at locations further than the tape approach to desired levels. The two devices are placed at points (1.2 1.2) and (1.2 1.6), respectively. Figure 12 shows the charging utility for three algorithms for $R_t = 105, 115, 125\text{ (mW/cm}^2\text{)}$ with $\eta = 0.7$ and $\epsilon = 0.15$. On average, Centralized ROSE and Distributed ROSE outperform Set-Cover by 480.19% and 391.09%, respectively. Such high gain is because Set-Cover happens to tune the first charger to its maximum power but yielding little charging utility, and leave little room to tune the left chargers which have higher charging efficiency. Moreover, we collected multiple samples at a location, and found the 70-*th* quantile value (as $\eta = 0.7$) as its reference EMR value. Figure 13 shows the measured reference EMR distribution in the area for our Centralized ROSE algorithm with $R_t = 125\text{ mW/cm}^2$. We can see that the peak EMR value is $94\text{ }\mu\text{W/cm}^2$, less than R_t .

VIII. CONCLUSION

The key novelty of this paper is on proposing the first scheme for robustly safe charging for wireless charger networks considering EMR jitter. The key contributions of this paper are establishing the empirical probabilistic charging model, developing both centralized and distributed approximation algorithms, and conducting both simulations and field experiments for evaluation. The key technical depth of this paper is in proposing the EMR approximation and area discretization methods to reformulate the problem into the classical problem of SOCP, developing the first centralized and distributed second-order cone constraint reduction schemes, and presenting the fully distributed algorithm and bounding its performance. Our simulations and experimental results show that our proposed scheme achieves good performance and can outperform comparison algorithms by 480.19%.

ACKNOWLEDGMENT

This work is partially supported by the National Natural Science Foundation of China under Grant Numbers 61502229, 61672353, 61472252, 61321491, 61629302, 61373130, 61672276, 61772265, and 61602194, China 973 projects (2014CB340303), the Joint Research Fund for Overseas Chinese Scholars and Scholars in Hong Kong and Macao Young Scholars F030307 under Grant Number 61629302, and National Science and Technology Major Project of China under Grant Number 2017ZX03001013-003.

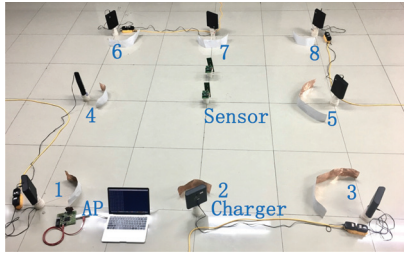


Fig. 11: Testbed

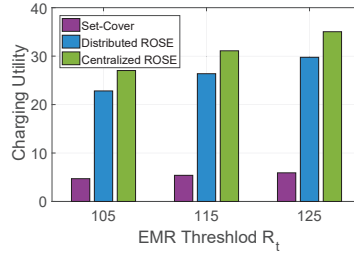


Fig. 12: Charging utility comparison

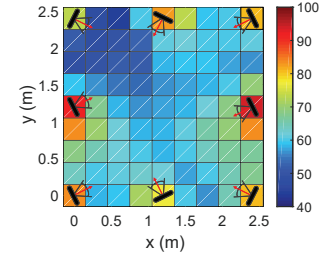


Fig. 13: Reference EMR distribution

REFERENCES

- [1] “<https://www.electronics.ca/store/wireless-power-transmission-market-forecast-analysis.html>.”
- [2] H. Dai *et al.*, “Safe charging for wireless power transfer,” in *IEEE INFOCOM*, 2014, pp. 1105–1113.
- [3] “<http://www.powercastsensors.com/category/applications/page/2/>.”
- [4] R. Zhang *et al.*, “Mimo broadcasting for simultaneous wireless information and power transfer,” *IEEE Transactions on Wireless Communications*, vol. 12, no. 5, pp. 1989–2001, 2013.
- [5] “<http://www.icnirp.org/cms/upload/publications/ICNIRPmfgdl.pdf>.”
- [6] “http://www.zhb.gov.cn/gkml/hbb/bgg/201410/t20141022_290444.htm.”
- [7] H. Dai *et al.*, “Safe charging for wireless power transfer,” *IEEE/ACM Transactions on Networking*, vol. 25, no. 6, pp. 3531–3544, 2017.
- [8] —, “SCAPE: Safe charging with adjustable power,” in *IEEE ICDCS*, 2014, pp. 439–448.
- [9] —, “SCAPE: Safe charging with adjustable power,” *IEEE/ACM Transactions on Networking*, 2018.
- [10] S. Nikolettseas *et al.*, “Low radiation efficient wireless energy transfer in wireless distributed systems,” in *IEEE ICDCS*, 2015, pp. 196–204.
- [11] H. Dai *et al.*, “Radiation constrained wireless charger placement,” in *IEEE INFOCOM*, 2016, pp. 1–9.
- [12] —, “Radiation constrained scheduling of wireless charging tasks,” in *ACM MobiHoc*, 2017, pp. 17–26.
- [13] —, “Radiation constrained scheduling of wireless charging tasks,” *IEEE/ACM Transactions on Networking*, 2018.
- [14] Lanlan *et al.*, “Radiation constrained fair wireless charging,” in *IEEE SECON*, 2017, pp. 1–9.
- [15] S. He *et al.*, “Energy provisioning in wireless rechargeable sensor networks,” *IEEE Transactions on Mobile Computing*, vol. 12, no. 10, pp. 1931–1942, 2013.
- [16] H. Dai *et al.*, “Omnidirectional chargability with directional antennas,” in *IEEE ICNP*, 2016, pp. 1–10.
- [17] —, “Optimizing wireless charger placement for directional charging,” in *IEEE INFOCOM*, 2017, pp. 2922–2930.
- [18] S. Boyd and L. Vandenberghe, *Convex optimization*. Cambridge university press, 2004.
- [19] N. M. Razali *et al.*, “Power comparisons of shapiro-wilk, kolmogorov-smirnov, lilliefors and anderson-darling tests,” *Journal of statistical modeling and analytics*, vol. 2, no. 1, pp. 21–33, 2011.
- [20] K. M. Rabie *et al.*, “Wireless power transfer in cooperative df relaying networks with log-normal fading,” in *IEEE GLOBECOM*, 2016, pp. 1–6.
- [21] —, “Energy-harvesting in cooperative af relaying networks over log-normal fading channels,” in *IEEE ICC*, 2016, pp. 1–7.
- [22] “http://www.epixanalytics.com/modelassist/AtRisk/Model_Assist.htm#Distributions/Approximations/Normal_approximation_to_the_Lognormal_distribution.htm.”
- [23] S. He *et al.*, “Energy provisioning in wireless rechargeable sensor networks,” in *IEEE INFOCOM*, 2011, pp. 2006–2014.
- [24] S. Ross, *A first course in probability*. Pearson, 2014.
- [25] R. G. Michael and S. J. David, “Computers and intractability: a guide to the theory of np-completeness,” *WH Free. Co., San Fr*, 1979.
- [26] Q. Peng *et al.*, “Distributed algorithm for optimal power flow on a radial network,” in *IEEE CDC*, 2014, pp. 167–172.

- [27] H. Dai *et al.*, “Using minimum mobile chargers to keep large-scale wireless rechargeable sensor networks running forever,” in *IEEE ICC-CN*, 2013, pp. 1–7.
- [28] —, “Minimizing the number of mobile chargers for large-scale wireless rechargeable sensor networks,” *Computer Communications*, vol. 46, pp. 54–65, 2014.
- [29] —, “Practical scheduling for stochastic event capture in wireless rechargeable sensor networks,” in *IEEE WCNC*, 2013, pp. 986–991.
- [30] —, “Impact of mobility on energy provisioning in wireless rechargeable sensor networks,” in *IEEE WCNC*, 2013, pp. 962–967.
- [31] —, “Quality of energy provisioning for wireless power transfer,” *IEEE Transactions on Parallel and Distributed Systems*, vol. 26, no. 2, pp. 527–537, 2015.
- [32] —, “Practical scheduling for stochastic event capture in energy harvesting sensor networks,” *International Journal of Sensor Networks*, vol. 18, no. 2, pp. 85–100, 2015.
- [33] N. Yu *et al.*, “Placement of connected wireless chargers,” in *IEEE INFOCOM*, 2018. To appear.
- [34] “www.powercastco.com.”
- [35] M. Voitsekhovskii, “Minkowski inequality,” *Hazewinkel, Michiel, Encyclopedia of Mathematics. Springer: The Netherlands*, 1997.

APPENDIX

A. Proof of Theorem 5.1

Proof: Suppose the obtained adjusting factor for charger s_i by our distributed algorithm is x_i , and the optimal adjusting factors for s_i for problem **P3** or **P2** (or **P1**) is x_i^* ; and the overall charging utilities corresponding to the three solutions are \mathcal{U} , \mathcal{U}^* , and \mathcal{U}^* , respectively. Suppose the computed adjusting factor for s_i for the turn-off strategy $\langle p, q \rangle$ is $x_i^{\langle p, q \rangle}$, and its corresponding charging utility is $\mathcal{U}^{\langle p, q \rangle}$. We first prove the feasibility of the obtained solution x_i ($x_i = \frac{\sum_{p=1}^M \sum_{q=1}^M x_i^{\langle p, q \rangle}}{M^2}$). Clearly, we have

$$\begin{cases} \sum_{i=1}^n \tilde{P}_{iz} x_i^{\langle 1, 1 \rangle} + \Phi^{-1}(\eta) \sqrt{\sum_{i=1}^n \tilde{\sigma}_{P,iz}^2 (x_i^{\langle 1, 1 \rangle})^2} \leq \frac{R_t}{c_e}, \\ \dots \dots \\ \sum_{i=1}^n \tilde{P}_{iz} x_i^{\langle M, M \rangle} + \Phi^{-1}(\eta) \sqrt{\sum_{i=1}^n \tilde{\sigma}_{P,iz}^2 (x_i^{\langle M, M \rangle})^2} \leq \frac{R_t}{c_e}, \end{cases}$$

where $z = 1, \dots, Z$. By summing up L.H.S. and R.H.S. of the M^2 inequalities and dividing both of them by M^2 , and plugging in $x_i = \frac{\sum_{p=1}^M \sum_{q=1}^M x_i^{\langle p, q \rangle}}{M^2}$, we have

$$\sum_{i=1}^n \tilde{P}_{iz} x_i + \frac{1}{M^2} \sum_{p=1}^M \sum_{q=1}^M \Phi^{-1}(\eta) \sqrt{\sum_{i=1}^n \tilde{\sigma}_{P,iz}^2 (x_i^{\langle p, q \rangle})^2} \leq \frac{R_t}{c_e}, \quad (19)$$

where $z = 1, \dots, Z$. Further, as per Minkowskis Inequality [35], for any $\mathbf{u}, \mathbf{v} \in \mathbb{R}^n$ and $p \in [1, +\infty)$, it holds that $\|\mathbf{u} + \mathbf{v}\|_p \leq \|\mathbf{u}\|_p + \|\mathbf{v}\|_p$. Here $\|\cdot\|_p$ indicates the ℓ_p -norm. Therefore, we have

$$\sqrt{\sum_{i=1}^n \tilde{\sigma}_{P,iz}^2 x_i^2} = \sqrt{\sum_{i=1}^n \tilde{\sigma}_{P,iz}^2 \left(\frac{1}{M^2} \sum_{p=1}^M \sum_{q=1}^M x_i^{\langle p, q \rangle} \right)^2}$$

$$\begin{aligned}
 &= \sqrt{\sum_{i=1}^n \left(\sum_{p=1}^M \sum_{q=1}^M \frac{\tilde{\sigma}_{P,iz} x_i^{<p,q>}}{M^2} \right)^2} \\
 &= \left\| \sum_{p=1}^M \sum_{q=1}^M \left(\frac{\tilde{\sigma}_{P,1z} x_1^{<p,q>}}{M^2}, \dots, \frac{\tilde{\sigma}_{P,nz} x_n^{<p,q>}}{M^2} \right) \right\|_2 \\
 &\leq \sum_{p=1}^M \sum_{q=1}^M \left\| \left(\frac{\tilde{\sigma}_{P,1z} x_1^{<p,q>}}{M^2}, \dots, \frac{\tilde{\sigma}_{P,nz} x_n^{<p,q>}}{M^2} \right) \right\|_2 \\
 &= \sum_{p=1}^M \sum_{q=1}^M \sqrt{\sum_{i=1}^n \left(\frac{\tilde{\sigma}_{P,iz} x_i^{<p,q>}}{M^2} \right)^2} \\
 &= \frac{1}{M^2} \sum_{p=1}^M \sum_{q=1}^M \sqrt{\sum_{i=1}^n \tilde{\sigma}_{P,iz}^2 (x_i^{<p,q>})^2} \quad (20)
 \end{aligned}$$

Note that the inequality at the fourth step in the above derivation is obtained by iteratively applying Minkowski's Inequality. By combining (19) and (20), we obtain

$$\begin{aligned}
 &\sum_{i=1}^n \tilde{P}_{iz} x_i + \Phi^{-1}(\eta) \sqrt{\sum_{i=1}^n \tilde{\sigma}_{P,iz}^2 x_i^2} \\
 &\leq \sum_{i=1}^n \tilde{P}_{iz} x_i + \frac{1}{M^2} \sum_{p=1}^M \sum_{q=1}^M \Phi^{-1}(\eta) \sqrt{\sum_{i=1}^n \tilde{\sigma}_{P,iz}^2 (x_i^{<p,q>})^2} \\
 &\leq \frac{R_t}{c_e} \quad (21)
 \end{aligned}$$

where $z = 1, \dots, Z$. This indicates that x_i s is a feasible solution to problem **P3**, as well as **P2** as per Lemma 4.2.

Next, assume we obtain in total K M -Clusters. Suppose the aggregated charging utility for the chargers in the cell lies in the i -th row and j -th column in the k -th M -Cluster in the optimal solution to **P3** is u_{ijk} . Moreover, suppose the aggregated charging utility included in the optimal charging utility to **P3** achieved by the chargers that are switched on (switched off) for the policy $\langle p, q \rangle$ is $\tilde{U}^{* \langle p, q \rangle}$ ($\bar{U}^{* \langle p, q \rangle}$). Evidently, we have

$$\bar{U}^{* \langle p, q \rangle} = \sum_{k=1}^K \left(\sum_{i=p}^M \sum_{j=1}^M u_{ijk} + \sum_{i=1}^M \sum_{j=q}^M u_{ijk} - u_{p,qk} \right). \quad (22)$$

Further, as $\mathcal{U}^{<p,q>}$ is optimal under the settings of the turn-off policy $\langle p, q \rangle$, then we have

$$\mathcal{U}^{<p,q>} \geq \tilde{U}^{* \langle p, q \rangle}. \quad (23)$$

As $\tilde{U}^{* \langle p, q \rangle} + \bar{U}^{* \langle p, q \rangle} = \tilde{U}^*$, we then obtain

$$\mathcal{U}^{<p,q>} + \bar{U}^{* \langle p, q \rangle} \geq \tilde{U}^*. \quad (24)$$

By enumerating all M^2 turn-off policies, we have

$$\sum_{p=1}^M \sum_{q=1}^M \mathcal{U}^{<p,q>} + \sum_{p=1}^M \sum_{q=1}^M \bar{U}^{* \langle p, q \rangle} \geq M^2 \tilde{U}^*. \quad (25)$$

Besides, it is clear that

$$\begin{aligned}
 &\sum_{p=1}^M \sum_{q=1}^M \bar{U}^{* \langle p, q \rangle} \\
 &= \sum_{p=1}^M \sum_{q=1}^M \left(\sum_{k=1}^K \left(\sum_{i=p}^M \sum_{j=1}^M u_{ijk} + \sum_{i=1}^M \sum_{j=q}^M u_{ijk} - u_{p,qk} \right) \right)
 \end{aligned}$$

$$\begin{aligned}
 &= \sum_{q=1}^M \left(\sum_{k=1}^K \sum_{i=1}^M \sum_{j=1}^M u_{ijk} \right) + \sum_{p=1}^M \left(\sum_{k=1}^K \sum_{i=1}^M \sum_{j=1}^M u_{ijk} \right) \\
 &\quad - \sum_{p=1}^M \sum_{q=1}^M \sum_{k=1}^K u_{p,qk} = (2M-1) \sum_{k=1}^K \sum_{i=1}^M \sum_{j=1}^M u_{ijk} = (2M-1) \tilde{U}^*. \quad (26)
 \end{aligned}$$

By combining (25) and (26), we obtain

$$\frac{\sum_{p=1}^M \sum_{q=1}^M \mathcal{U}^{<p,q>}}{M^2} \geq \left(1 - \frac{2M-1}{M^2}\right) \tilde{U}^*. \quad (27)$$

Therefore, the achieved utility of our solution \mathcal{U} satisfies

$$\begin{aligned}
 \mathcal{U} &= c_u \sum_{i=1}^n \sum_{j=1}^m \bar{P}(d(s_i, o_j)) x_i \\
 &= c_u \sum_{i=1}^n \sum_{j=1}^m \bar{P}(d(s_i, o_j)) \frac{\sum_{p=1}^M \sum_{q=1}^M x_i^{<p,q>}}{M^2} \\
 &= \frac{\sum_{p=1}^M \sum_{q=1}^M c_u \sum_{i=1}^n (\sum_{j=1}^m \bar{P}(d(s_i, o_j))) x_i^{<p,q>}}{M^2} \\
 &= \frac{\sum_{p=1}^M \sum_{q=1}^M \mathcal{U}^{<p,q>}}{M^2} \geq \left(1 - \frac{2M-1}{M^2}\right) \tilde{U}^* \\
 &= (1 - \epsilon/2) \tilde{U}^*. \quad (\because m = \left\lceil \frac{1 + \sqrt{1 - \epsilon/2}}{\epsilon/2} \right\rceil) \quad (28)
 \end{aligned}$$

Further, we consider the optimal solution x_i^* to problem **P2**, apparently it satisfies

$$\begin{aligned}
 &\sum_{i=1}^n \bar{P}(d(s_i, p)) x_i^* + \Phi^{-1}(\eta) \sqrt{\sum_{i=1}^n \sigma_P^2(d(s_i, p)) (x_i^*)^2} \leq \frac{R_t}{c_e}, \\
 &\forall p \in \mathbb{R}^2, 0 \leq x_i \leq 1 \quad (i = 1, \dots, n). \quad (29)
 \end{aligned}$$

Consider an arbitrary point p which lies in the z -th subarea. Further, as per Lemma 4.1, when we set both the approximation error thresholds for EMR expectation and standard deviation, i.e., ϵ_1 and ϵ_2 , as $\epsilon/2$, we have $\frac{\tilde{e}(d)}{\bar{e}(d)} = \frac{\tilde{P}_{iz}(d)}{\bar{P}(d(s_i, p))} \leq 1 + \epsilon/2$ and $\frac{\tilde{\sigma}_e(d)}{\sigma_e(d)} = \frac{\tilde{\sigma}_{P,iz}}{\sigma_P(d(s_i, p))} \leq 1 + \epsilon/2$, and therefore

$$\begin{aligned}
 &\sum_{i=1}^n \tilde{P}_{iz} \left(\frac{x_i^*}{1 + \epsilon/2} \right) + \Phi^{-1}(\eta) \sqrt{\sum_{i=1}^n \tilde{\sigma}_{P,iz}^2 \left(\frac{x_i^*}{1 + \epsilon/2} \right)^2} \\
 &= \sum_{i=1}^n \left(\frac{\tilde{P}_{iz}}{1 + \epsilon/2} \right) x_i^* + \Phi^{-1}(\eta) \sqrt{\sum_{i=1}^n \left(\frac{\tilde{\sigma}_{P,iz}}{1 + \epsilon/2} \right)^2 (x_i^*)^2} \\
 &\leq \sum_{i=1}^n \bar{P}(d(s_i, p)) x_i^* + \Phi^{-1}(\eta) \sqrt{\sum_{i=1}^n \sigma_P^2(d(s_i, p)) (x_i^*)^2} \\
 &\leq \frac{R_t}{c_e}, \quad (30)
 \end{aligned}$$

which implies $\frac{x_i^*}{1 + \epsilon/2}$ is a feasible solution to the problem **P3**.

As \tilde{U}^* is the optimal solution to **P3**, we thus have

$$\begin{aligned}
 \tilde{U}^* &\geq c_u \sum_{i=1}^n \sum_{j=1}^m \bar{P}(d(s_i, o_j)) \frac{x_i^*}{1 + \epsilon/2} \\
 &\geq \frac{1}{1 + \epsilon/2} c_u \sum_{i=1}^n \sum_{j=1}^m \bar{P}(d(s_i, o_j)) x_i^* \\
 &\geq \frac{1}{1 + \epsilon/2} \mathcal{U}^* \geq (1 - \epsilon/2) \mathcal{U}^*.
 \end{aligned}$$

Combining Equations (28) and (31), we have

$$\mathcal{U} \geq (1 - \epsilon/2) \cdot (1 - \epsilon/2) \mathcal{U}^* \geq (1 - \epsilon) \mathcal{U}^*. \quad (31)$$

Thus, our algorithm achieves $(1 - \epsilon)$ -approximation ratio. We omit the communication delay analysis to save space. \blacksquare